High Luminosity Options for the JLC/NLC at 500 GeV cms

T.O. Raubenheimer and K.A. Thompson

LCC–0004

June 16, 1998

1 Introduction

The present JLC/NLC parameters are chosen to provide luminosities between $0.5 \sim 0.75 \times 10^{34}\, s^{-1}\, cm^{-2}$ at a cms energy of 500 GeV [1]; the parameters are listed in Table 1 for both the 500 GeV and 1 TeV cases. In all cases, these luminosities assume extensive margins and emittance dilutions to ensure that they are attainable. In this note, we consider the feasibility of substantially higher luminosities which might be attained by operating with smaller emittance dilutions and higher beam currents. The parameters we will describe are listed in Table 2 where these high luminosity sets (ILC-IHa and ILC-IHb) are compared with the base JLC/NLC set (ILC-Ib) and with the high luminosity TESLA parameter set. In the next sections, we will discuss the limitations and assumptions leading to these higher luminosity parameter sets. The details in our discussion will be based on the NLC design described in the Zeroth-order Design Report (ZDR) but the same arguments, with slightly different values, could be applied to the JLC reference design.

2 Beam Current

The nominal JLC/NLC parameters are based on a 2.8ns bunch spacing which is twice the 1.4ns bunch spacing specified in the NLC ZDR. The larger bunch spacing was adopted to take advantage of a longer klystron pulse and reduce

Table 1. IP and linac parameters for the ILC

	500 GeV			1 TeV		
	A	B	C	A	B	C
CMS Energy (GeV)	520	500	480	1050	1000	950
Luminosity w/ IP dilutions (10^{33})	7.5	6.25	5.0	15	12.5	10
Repetition Rate (Hz)		120			120	
Bunch Charge (10^{10})	0.8	1.0	1.15	0.8	1.0	1.15
Bunches/RF Pulse		87			87	
Bunch Separation (ns)		2.8			2.8	
Injected $\gamma\varepsilon_x/\gamma\varepsilon_y$ (10^{-8}m-rad)		300 / 3			300 / 3	
$\gamma\varepsilon_x$ at IP (10^{-8}m-rad)	400	500	600	400	500	600
$\gamma\varepsilon_y$ at IP (10^{-8}m-rad)	6	10	14	6	10	14
β_x/β_y at IP (mm)	10/0.100	12/0.125	14/0.200	10/0.125	12/0.160	14/0.200
σ_x/σ_y at IP (nm)	280/3.5	350/5.1	422/7.7	197/2.8	247/4.1	300/5.5
σ_z at IP (μm)	100	125	150	100	125	150
Υ (Beamstrahlung Param.)	0.13	0.10	0.08	0.39	0.30	0.22
Pinch Enhancement	1.38	1.36	1.47	1.50	1.47	1.48
Beamstrahlung δ_B (%)	4.4	4.0	2.9	11.9	10.3	8.4
# Photons per e^-/e^+	1.10	1.17	1.10	1.45	1.50	1.45
Rf overhead (%)		8			8	
Average rf phase (deg.)	10.6	11.7	13.0	10.9	11.4	13.1
Linac Tolerances (μm)	16.1	15.2	14.6	13.1	11.7	11.9
Unloaded Gradient (MV/m)		77			77	
Effective Gradient† (MV/m)	59.7	56.7	54.5	59.7	56.7	54.5
Active Linac Length (km)		4.3			8.9	
Power/Beam (MW)	3.4	4.2	4.6	7.1	8.4	9.3
# of Structures per linac		2376			4968	
Structure Length (m)		1.8			1.8	
Structure Iris (a/λ)		0.171			0.171	
Structure Atten. (τ)		0.54			0.54	
Shunt Impedance (MΩ/m)		95			95	
Fill Time (ns)		118			118	
Q		7800			7800	
# of Klystrons per linac		1584			3312	
Klystron Peak Pwr. (MW)		75			75	
Klystron Pulse Length (μs)		1.5			1.5	
Pulse Method		4/4 DLDS			4/4 DLDS	
Pulse Comp. Gain (85% eff.)		3.4			3.4	
RF System Efficiency (%)		38			38	
Total AC Power (MW)		94			191	

† Effective gradient includes rf overhead (8%) and average rf phase $\cos\overline{\phi}_{rf}$.

Table 2. High luminosity parameters for JLC/NLC and TESLA

	ILC-Ib	ILC-IHa	ILC-IHb †	TESLA[2]
Nominal CMS Energy (TeV)	0.5		0.5	
Luminosity without pinch (10^{33})	3.9	10.4	15.8	16.2
Pinch Enhancement (H_D) ‡	1.42	1.36	1.30	1.61
H_D (w/ waist shift) *	1.46	1.50	1.40	1.93
H_D (w/ waist shift and offset) ¶	1.32	1.14	1.18	0.98
Luminosity (10^{33}) §	6.3	12.1	17.5	31.0
Repetition Rate (Hz)	120	120	120	5
Bunch Charge (10^{10})	1.0	1.0	0.75	2.0
Bunches/RF Pulse	90	90	90	2820
Bunch Separation (ns)	2.8	2.8	1.4	337
$\gamma\varepsilon_{x,y}$ at DR (10^{-8}m-rad)	300 / 3	300 / 2	300 / 2	800 / 2
$\gamma\varepsilon_{x,y}$ at IP (10^{-8}m-rad)	500 / 10	400 / 3	400 / 3	1000 / 3
β_x/β_y at IP (mm)	12/0.125	13/0.100	10/0.080	15/0.400
σ_x/σ_y at IP (nm)	350/5.1	324/2.5	287/2.2	553/5.0
σ_z at IP (μm)	125	115	85	400
Linac Tolerances $^{\|}$ (μm)	14.6	7.1	10.5	500
Υ (Beamstrahlung Param.)	0.10	0.13	0.34	0.05
Beamstrahlung δ_B (%)	4.0	5.1	4.6	3.1
# Photons per e^-/e^+	1.2	1.3	1.1	1.9

$\dagger$ For the same cms energy, the ILC-IHb is 10% longer than the nominal ILC design because of the higher beam loading

$\ddagger$ Guinea Pig simulation for the luminosity enhancement — the analytic result is very close to these values

$\star$ Enhancement from Guinea Pig simulations assuming that the e^+/e^- waists are offset by $1.6\sigma_z$ — this optimizes the enhancement

$\P$ Enhancement with waist shift and a vertical offset of $1\sigma_y$ which allows an estimation of the kick instability

$\S$ In the ILC designs, the luminosity is estimated including both the waist shift and a 1σ transverse offset of the beams while in the TESLA case the luminosity was estimated with the waist shift but assuming perfect head-on collisions; because of the large disruption, the TESLA luminosity decreases to $\mathcal{L} = 17 \times 10^{33}$ if a 1σ transverse offset is included.

$\|$ Tolerances calculated assuming that 50% of the total emittance budget is used by dilutions from short-range transverse wakefields.

Table 3. Luminosity spectra for JLC/NLC and TESLA

	ILC-Ib	ILC-IHa	ILC-Hb	TESLA
Total Luminosity	0.5	0.5	0.45	0.5
Luminosity at 100% E_{cms}	42%	40%	46%	33%
Luminosity within 99% E_{cms}	69%	66%	70%	70%
Luminosity within 95% E_{cms}	89%	86%	88%	93%

the beam loading, thereby, reducing the number of klystron power sources required to attain the full beam energy.

In this note, we consider two cases: ILC-IHa and ILC-IHb. The former assumes the same beam current as the nominal parameters ILC-Ib (Table 1) but with reduced beam emittances while the later assumes a current that is roughly 50% higher and approaches that specified in the ZDR as well as the reduced emittances. This higher current solution will have larger beam loading and, assuming the same klystron population, would have a final energy that is roughly 10% lower than nominal. However, because of the lower single bunch charge, the tolerances will be looser than in ILC-IHa. Furthermore, because of the higher beam current, the luminosity will be higher than in ILC-Ia. The current specified in ILC-IHb is 10% lower than the maximum current the sources are presently specified to produce and thus the charge margins are signifcantly lower than in the present design or the ILC-IHa parameters.

3 Emittance Generation

The initial beam emittances are determined by the damping rings. The present parameter sets specify extracted emittances of $\gamma\epsilon_{x,y} = 3$mm-mrad and 0.03mm-mrad. In the NLC damping rings, the extracted $\gamma\epsilon_x$ is essentially equal to the equilibrium emittance in the ring; this is determined by the damping ring optics and the intrabeam scattering. In contrast, roughly 25% of the extracted $\gamma\epsilon_y$ is due to the injected emittance and while the remainder comes from the equilibrium value which is primarily determined by the alignment errors causing vertical dispersion and betatron coupling; the synchrotron radiation opening angle contribution to the vertical emittance is roughly an order-of-magnitude smaller and can be neglected. It should be straightforward to attain smaller vertical equilibrium emittances by reducing the alignment errors. As discussed in the ZDR, after using two skew quadrupoles to correct the residual disperion, the equilibrium vertical emittance has an *expected* value of 0.014mm-mrad and a 95% confidence of being less than 0.030mm-mrad. Additional skew elements could be used reduce both the expected value and the tails of the distribution, however it is probably easiest to directly reduce the errors.

The most important errors are the verical misalignments of the sextupoles which were specified to have an rms of 50μm. In the ZDR, it was noted that, with orbit bumps of 250μm, beam-based techniques should be able to attain sextupole alignment better than 20μm. Assuming a reduction of the rms sextupole misalignments from 50μm to 30μm would yield an expected extracted $\gamma\epsilon_y$ of roughly 0.012mm-mrad with a 95% confidence of attaining a value less than 0.020mm-mrad. Although studies have not yet been performed on the required stability, this would seem to be a reasonable performance expectation.

This smaller vertical emittance will increase the density dependent effects such as intrabeam scattering and the space charge tune shifts. In the ZDR, the intrabeam scattering was calculated for a bunch charge of 1.5×10^{10} while the present parameters specify $< 1.0 \times 10^{10}$. At the lower charge and emittance, the emittance growth due to IBS will be similar to that calculated for the ZDR and thus is not a limitation. Similary, the space charge tune shift for the ZDR parameters was $\Delta\nu_y \approx 0.03$ and it is not significantly different for these low emittance parameters because of the lower bunch charge.

4 Emittance Transport

In the ILC-I parameters, we have assumed relatively large emittance dilutions during the acceleration and transport to the IP while in the ILC-IH parameters we have assumed relatively small dilutions. The ILC-I dilutions are based on the assumption that emittance correction techniques are not used. In the main linacs, only the trajectory is corrected and the accelerator structures are aligned to the trajectory using rf BPM's and movers.

The primary source of emitance dilution is the short-range transverse wakefields in the main linacs. At this time, we do not know the full capabilities of the rf bpm system which will be used to align the structures and, although the ideal accuracy should be sub-micron, systematic errors will likely degrade the performance. For this reason, we have assumed relatively loose alignment tolerances. In addition, allowing for large dilutions will allow rapid commissioning of the collider and will simplify operation while the more advanced correction techniques can be studied and tested. However, emittance correction techniques are demonstrated repeatedly in the SLC. Simple bump-type corrections can be expected to reduce the dilutions from hundreds of percent to a few tens of percent as they do in the SLC *provided* the beam emittances can be measured. The laser wire system proposed for the JLC/NLC should have no problem resolving the linac beam sizes, even with these reduced emittances.

Thus, to estimate the IP emittances for the high luminosity parameters, we assume that the dilutions are corrected and remain at 30% in the horizontal and 50% in the vertical. For scale, Table 2 lists the accelerator structure alignment tolerance that would needed to limit the vertical emittance dilution due to the short-range transverse wakefield in the main linac to 25%. This tolerance is about 2 to 3 times smaller than for the nominal parameters but it is still within the expected performance of the rf bpms and thus these emittances may be attainable even without extensive emittance correction.

5 Bunch Length and IP Beta Functions

The high luminosity parameters assume a bunch length which is $10 \sim 20\%$ smaller than in the nominal parameters. The bunch length is reduced to decrease the effect of the transverse wakefields and allow for smaller IP beta functions. However, the longitudinal wakefield becomes more difficult to compensate by running off the rf-crest. To attain an energy spectrum of 0.8% FWHM at the entrance to the final focus with the high luminosity parameters, either the average rf phase must be increased to about 15 degrees as compared to about 12 degrees in the nominal parameters or bunch shaping techniques, similar to those used in the SLC, must be adopted. The smaller bunch length could be attained by slightly increasing the rf voltage in the 2nd bunch compressor.

With the shorter bunch length, it is reasonable to consider reduced vertical IP beta functions. The smaller IP beta functions imply larger chromaticity and larger beta functions through the rest of the final focus. However, with the smaller beam emittances, the beam stay-clear and the geometric and chromo-geometric aberations are thought to be comparable to those in the base design.

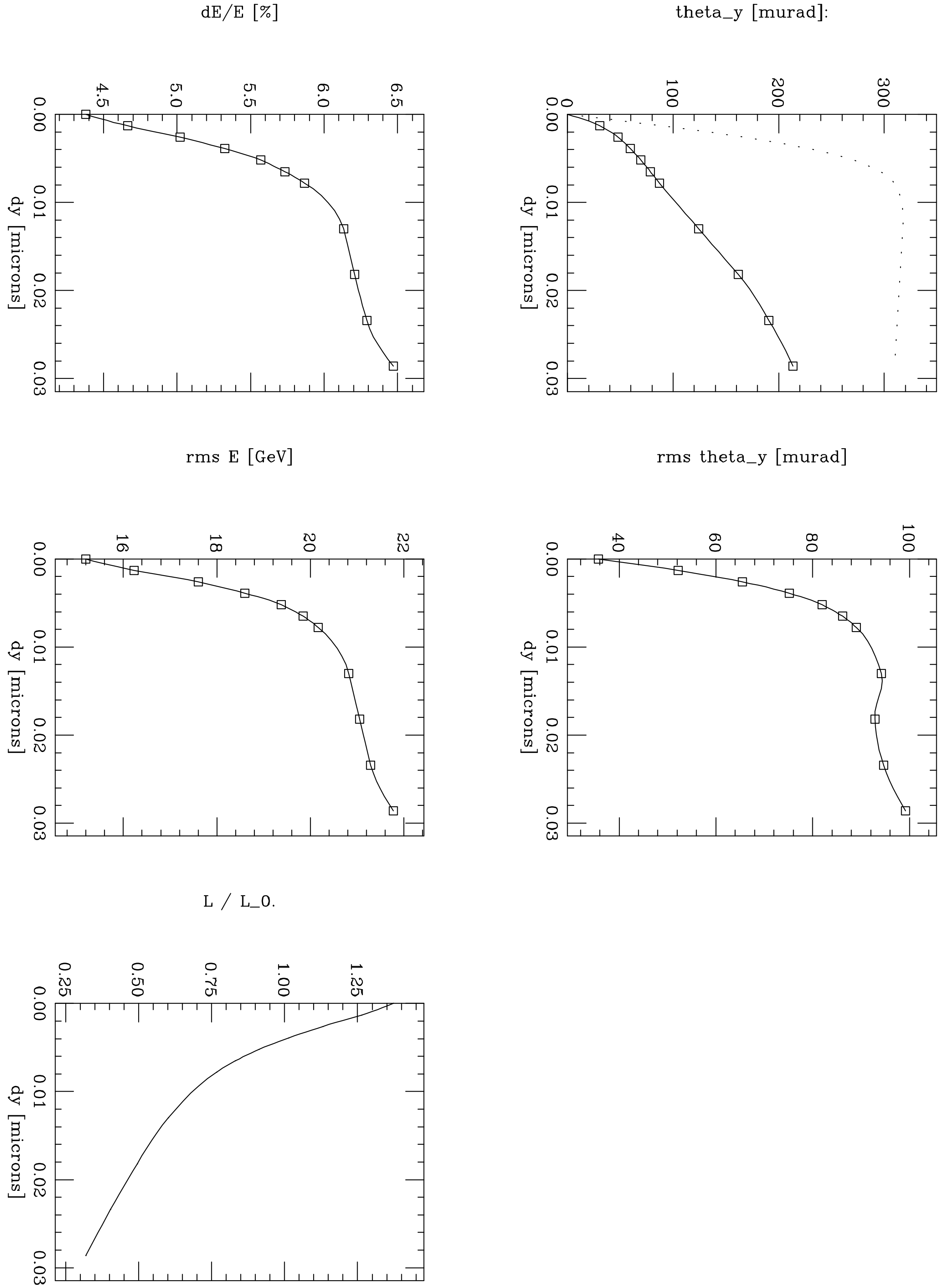

Figure 1: Outgoing angular distribution, average and rms energy loss, and luminosity versus offset between colliding beams with ILC-IHa parameters

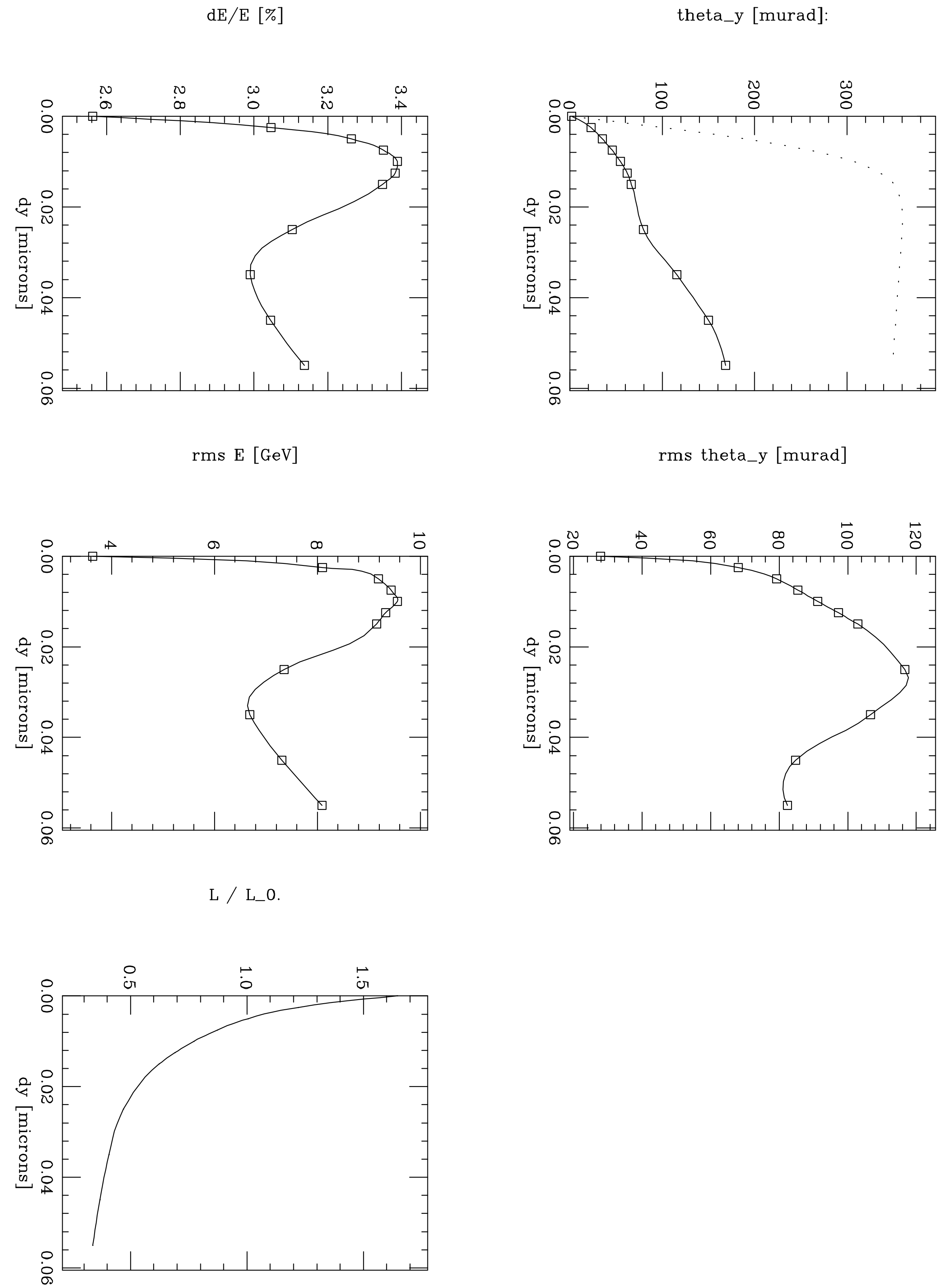

Figure 2: Outgoing angular distribution, average and rms energy loss, and luminosity versus offset between colliding beams with TESLA parameters

6 Beam-Beam Effects and Spectrum

With the smaller beam emittances, the beam-beam disruption $D_y \approx 12 \sim 16$ is much larger than with the nominal parameters. The disruption effects are illustrated in Figures 1 and 2 which correspond to the ILC-IHa and the TESLA parameters, respectively. In the figures, the outgoing angular distributions, the energy loss due to beamstrahlung, and the luminosity, calculated by the simulation code GuineaPig, are plotted versus the offset between the colliding bunches.

Another problem arises at high disruptions where the kink instability causes the luminosity to decrease rapidly as the beams are offset. The effect of the kink instability can be seen in the rapid decrease of the luminosity versus the offset between the colliding bunches illustrated in Figures 1 and 2. In the nominal JLC/NLC parameters, this does not yet appear to be a limitation; the luminosity only decreases by 9% when the beams are offset by σ_y. However, because the beams will jitter from pulse-to-pulse, it is probably reasonable to assume a luminosity enhancement equal to that calculated when the beams are offset by σ_y; this enhancement will include any increased sensitivity due to the kink instability. The final values listed in Table 2 include this offset the colliding beams.

Another issue, that may be important at high disruption, is the reduced sensitivity of the beam-beam deflection scans. This may make the operation of tuning and alignment feedback systems more difficult. At this time, we cannot evaluate this impact.

Finally, the luminosity spectra of the different designs is compared in Table 3. Note that although the average energy loss due to beamstrahlung may be higher in the high luminosity cases, close to the full center-of-mass energy the spectra are very similar; this arises because the expected number of photons radiated per electron is similar.

7 Summary

We have discussed parameters for the ILC that would yield luminosities two to three times larger than in the nominal design. The primary changes are: (1) smaller IP emittances which are likely possible using emittance correction techniques, (2) shorter bunch lengths and smaller IP beta functions which do not have a significant impact on the tolerances or requirements of the system, and, for the largest increase, (3) a bunch spacing of 1.4 ns rather than 2.8 ns.

These changes combined would yield a luminosity in excess of $\mathcal{L} > 20 \times 10^{33}\,\mathrm{cm}^{-2}\,\mathrm{s}^{-1}$. However, because of the larger disruption with these parameters, the kink instability has a greater impact and will make the resulting luminosity very sensitive to offsets between the colliding beams. Assuming beam offsets of 1σ, the kink instability will drease the luminosity by 15 to 20% to $\mathcal{L} \approx 17 \times 10^{33}\,\mathrm{cm}^{-2}\,\mathrm{s}^{-1}$.

References

[1] T.O. Raubenheimer, K. Yokoya, "Parameters for the JLC/NLC," LCC-Note-0003, 6/98.

[2] R. Brinkmann, presentation at March 98 TESLA collaboration meeting.